

Correspondence between dissipative phase transitions of light and time crystals

Fabrizio Minganti,^{1,*} Ievgen I. Arkhipov,^{2,†} Adam Miranowicz,^{1,3,‡} and Franco Nori^{1,4,§}

¹*Theoretical Quantum Physics Laboratory, RIKEN Cluster for Pioneering Research, Wako-shi, Saitama 351-0198, Japan*

²*Joint Laboratory of Optics of Palacký University and Institute of Physics of CAS, Faculty of Science, Palacký University, 17. listopadu 12, 771 46 Olomouc, Czech Republic*

³*Faculty of Physics, Adam Mickiewicz University, 61-614 Poznań, Poland*

⁴*Physics Department, The University of Michigan, Ann Arbor, Michigan 48109-1040, USA*

(Dated: March 17, 2024)

We predict the emergence of a time crystal generated by an incoherently driven and dissipative nonlinear optical oscillator, where the nonlinearity also comes from dissipation. We show that a second-order dissipative phase transition of light occurs in the frame rotating at the cavity frequency, while a boundary (dissipative) time crystal emerges in the laboratory frame. We relate these two phenomena by using the Liouvillian superoperator associated to the Lindblad master equation and its symmetries. These results connect the emergence of a second-order dissipative phase transition and a dissipative time crystal in the thermodynamic limit, allowing to interpret them as the same phenomenon in terms of the Liouvillian spectrum, but just in different frames.

I. INTRODUCTION

Correspondences play a central role in physics. Seminal examples include the bulk-edge correspondence, linking the presence of edge states to bulk topological invariants [1], and the AdS/CFT (gauge/gravity) correspondence, which establishes a duality between conformal field theories and supergravity [2]. Correspondences characterize related but yet different features of systems by linking their seemingly different properties. This article discusses the correspondence of two nonanalytical phenomena in open many-body quantum physics: *dissipative* phase transitions (DPTs) [3–5] and *boundary* [6] time crystals (BTCs) [7, 8].

The driven-dissipative physics of light is the focus of intense research, fostered by the achievements of non-negligible photon-photon interactions and sizeable light-matter couplings [9, 10]. Nonlinear resonators can be realized, e.g., in semiconductor microcavities [11] and superconducting circuits [12–14]. These systems are driven out of their thermal equilibrium and do not obey the paradigms of thermodynamics [15, 16]. Even in the absence of free-energy analysis, open quantum systems display critical phenomena, such as DPTs [5]. These out-of-equilibrium phases were initially studied in connection with lasing-like phenomena [17–20]. More recently, several examples of DPTs have been predicted for nonlinear optical systems [21–27] and spin systems [3, 28–37]. Experimentally, DPTs have been observed in lattices of superconducting resonators [38], Rydberg atoms in optical lattices [39, 40], optomechanical systems [41, 42], exciton-polariton condensates [9, 43], single superconducting cavities [44], and semiconductor micropillars [4, 45].

While a DPT is associated with the emergence of multiple steady states, a BTC is formed when permanent oscillations arise spontaneously in an otherwise time-translation invariant system [7, 46–50] (we will *not* consider discrete time crystals in time-dependent systems, where oscillations develop at times which are multiples of the driving one [51–53]). Questions concerning the resilience of BTCs in extended lattice geometries including generalized noise have been raised [46, 47], and the connection between the crystalline phase and the symmetries of the related model has been partially explored [8, 48, 49, 52, 54, 55].

In many of the previous works, the physics is captured by a Lindblad master equation. DPTs and BTCs can be understood as critical spectral properties of the Liouvillian superoperator, i.e., the matrix describing the evolution of the density matrix written in its vectorized form. A DPT emerges when one (or more) Liouvillian eigenvalues become zero in both real and imaginary parts [5, 56]. Similarly, for BTCs, the Liouvillian acquires eigenvalues with zero real part but nonzero imaginary one [7, 46, 57].

In this article, we study the correspondence between DPTs and BTCs by investigating a single-mode cavity with incoherent drive and incoherent nonlinear dissipative processes [26, 58, 59]. Using a simple change-of-reference transformation, we show that in the frame rotating at the cavity frequency (say, the R-frame) the system displays typical features of a DPT, while in the laboratory frame (the L-frame) the system undergoes time crystallization. Note that the Liouvillian is time-independent in both frames. Hence, we prove that for this highly-symmetrical model, a *second-order DPT and a BTC are one and the same phenomenon but in two different reference frames*. We stress that this fact can be seen as a proof of the existence of BTCs in open systems.

The article is structured as follows. In Sec. II we introduce a single-mode cavity with incoherent drive and incoherent nonlinear dissipative processes. We detail its master equation and the associated Liouvillian superoperator in the L-frame. We discuss the L-frame Liouvillian

* fabrizio.minganti@riken.jp

† ievgen.arkhipov@upol.cz

‡ miran@amu.edu.pl

§ fnori@riken.jp

lian properties and we show how to obtain the R-frame Liouvillian. We also briefly recall the main properties of time crystals and dissipative phase transitions. In Sec. III we numerically demonstrate the correspondence between BTCs and DPTs for the model under consideration. In Sec. IV we show the same correspondence but in a different nonlinear system, i.e., the Scully-Lamb laser model. We derive our conclusion in Sec. V.

II. THE MODEL

Hereafter, we consider the Hamiltonian $\hat{H} = \omega_c \hat{a}^\dagger \hat{a}$ of a harmonic oscillator (e.g., that of an optical cavity), where \hat{a} (\hat{a}^\dagger) is the bosonic annihilation (creation) operator. This system interacts with a weak Markovian environment, and its state is captured by a density matrix $\hat{\rho}(t)$ evolving under a Lindblad master equation ($\hbar = 1$)

$$\frac{d}{dt}\hat{\rho}(t) = \mathcal{L}\hat{\rho}(t) = -i[\hat{H}, \hat{\rho}(t)] + \sum_j \mathcal{D}[\hat{L}_j]\hat{\rho}(t). \quad (1)$$

Here, \mathcal{L} is the Liouvillian superoperator [15, 16], while $\mathcal{D}[\hat{L}_j]$ are the so-called Lindblad dissipators, whose action is

$$\mathcal{D}[\hat{L}_j]\hat{\rho}(t) = \hat{L}_j\hat{\rho}(t)\hat{L}_j^\dagger - \frac{\hat{L}_j^\dagger\hat{L}_j\hat{\rho}(t) + \hat{\rho}(t)\hat{L}_j^\dagger\hat{L}_j}{2}. \quad (2)$$

The operators \hat{L}_j are called jump operators and they describe how the environment acts on the system inducing loss and gain of bosons, energy, and information. In the following, we consider

$$\hat{L}_1 = \sqrt{\Gamma}\hat{a}, \quad \hat{L}_2 = \sqrt{\eta}\hat{a}^2, \quad \hat{L}_3 = \sqrt{\xi}\hat{a}^\dagger, \quad (3)$$

where \hat{L}_1 represents the single-particle loss, \hat{L}_2 the simultaneous loss of two photons, and \hat{L}_3 the incoherent drive (gain). The parameter Γ is the inverse of the photon lifetime, ξ represents the medium gain (incoherent drive) strength, and η is the two-photon dissipation rate. Such a model can be realized, e.g., considering an engineered thermal drive [26, 58] in the presence of an engineered two-photon dissipation [60, 61].

The system exhibits a $U(1)$ symmetry since any transformation $\hat{a} \rightarrow \hat{a}\exp(i\phi)$ for an arbitrary real number ϕ leaves Eq. (1) unchanged (see Appendix A). While Noether's theorem implies the presence of a conserved quantity for $U(1)$ Hamiltonian symmetries, this is not the case for the Liouvillian under consideration. Indeed, $U(1)$ is a weak symmetry of Eq. (1) and the extension of Noether's theorem for open systems require a strong symmetry [62–64]. Nonetheless, a Liouvillian symmetry constrains the dynamics of the system and influence its DPT [5].

A. Liouvillian spectrum

A central role in the following discussion is played by the steady state $\hat{\rho}_{ss}$, i.e., the matrix which is stationary under the action of the Liouvillian: $\partial_t \hat{\rho}_{ss} = \mathcal{L}\hat{\rho}_{ss} = 0$. For the system under consideration, if $\eta > 0$ there is a unique steady state and, therefore, $\hat{\rho}_{ss} = \lim_{t \rightarrow \infty} \hat{\rho}(t)$. The dynamics of the system cannot be obtained from the steady state alone. Having introduced the Liouvillian \mathcal{L} , we define its eigenvalues λ_i (representing typical decay times) and eigenmatrices $\hat{\rho}_i$ (encoding the states explored along the dynamics) via

$$\mathcal{L}\hat{\rho}_i = \lambda_i\hat{\rho}_i. \quad (4)$$

We order the eigenvalues λ_i in such a way that $|\text{Re}[\lambda_0]| < |\text{Re}[\lambda_1]| < \dots < |\text{Re}[\lambda_n]| < \dots$, i.e., the eigenvalues are ordered by their real part. In this regard, the steady state is proportional to $\hat{\rho}_0$, i.e., the eigenmatrix of the Liouvillian associated to $\lambda_0 = 0$. In the following, we will use QuTiP [65, 66] to numerically diagonalize the Liouvillian and obtain its eigenvalues and eigenmatrices.

B. Rotating frame of reference

The Hamiltonian dependence of the Liouvillian is eliminated in the frame which rotates at the cavity frequency ω_c . The density matrix in the R-frame becomes

$$\hat{\rho}^R(t) = \exp(i\omega_c t \hat{a}^\dagger \hat{a}) \hat{\rho}(t) \exp(-i\omega_c t \hat{a}^\dagger \hat{a}). \quad (5)$$

Since all the dissipators in Eq. (3) are $U(1)$ -symmetric, they are unchanged by the transformation. Hence, the Liouvillian \mathcal{L}^R in the R-frame, defined by $\partial_t \hat{\rho}^R(t) = \mathcal{L}^R \hat{\rho}^R(t)$, is simply

$$\mathcal{L}^R \hat{\rho}^R(t) = \sum_{j=1}^3 \mathcal{D}[\hat{L}_j] \hat{\rho}^R(t), \quad \mathcal{L}^R \hat{\rho}_i^R = \lambda_i^R \hat{\rho}_i^R, \quad (6)$$

where λ_i^R and $\hat{\rho}_i^R$ are its eigenvalues and eigenvectors, respectively. We stress two facts: (i) that both \mathcal{L}^R and \mathcal{L} are time independent; and (ii) the role of the symmetry in obtaining Eq. (6).

Normally, there is no trivial correspondence between λ_i^R and λ_i , or $\hat{\rho}_i$ and $\hat{\rho}_i^R$, due to the presence of “centrifugal forces” in the non-inertial R-frame. However, for the model under consideration one can explicitly compute $\mathcal{L}\hat{\rho}_i^R$, and using the presence of a $U(1)$ symmetry demonstrate that there exist the following fundamental relations (the proof is provided in Appendix B)

$$\hat{\rho}_i = \hat{\rho}_i^R, \quad \lambda_i = \lambda_i^R - i\omega_c k, \quad (7)$$

where k is an integer.

C. Dissipative phase transitions and Boundary time crystals

A DPT is a discontinuous change in the steady-state density matrix $\hat{\rho}_{\text{ss}}$ of a time-independent open quantum system as a function of a parameter ξ , i.e., at the critical point ξ_c , $\partial_{\xi}^n \hat{\rho}_{\text{ss}}(\xi_c) = \infty$ for some integer n . Similarly to a closed quantum system, where the Hamiltonian energy gap vanishes at the critical point of a quantum phase transition, in a DPT the Liouvillian gap closes [5, 48]. Symmetries are pivotal in understanding second-order (i.e., $n = 2$) DPTs [5, 37]. For a second-order DPT triggered by a spontaneous symmetry-breaking, several eigenvalues close simultaneously (one for each generator of the symmetry group except the identity). For example, the DPT associated to a Z_N symmetry breaking requires $\lambda_1 = \lambda_2 = \dots = \lambda_{N-1} = 0$ [5]. This corresponds to the emergence of N symmetry-breaking steady-state density matrices. For the $U(1)$ model under consideration, in the case of spontaneous symmetry breaking we expect infinitely-many eigenvalues to become zero.

Similarly, we can interpret BTCs as a critical phenomenon. Namely, given a time-independent Liouvillian \mathcal{L} which admits a unique steady state, a BTC appears in the thermodynamic limit if a characteristic frequency Ω appears such that the lowest-lying Liouvillian eigenvalues become $\lambda_{1,2} = \pm i\Omega$. In the same way in which a crystal breaks the spatial translation invariance, \mathcal{L} breaks the time-translation invariance at $t \rightarrow \infty$ and it develops everlasting oscillations for an observable whose time dynamics is ruled by $\lambda_{1,2}$. There are several definitions of time crystals for closed [51, 67], coherently driven [51, 68–70], and incoherently driven systems [47]. We focus on the diagnostic of BTCs based on the Liouvillian gap [7].

III. NUMERICAL STUDY

A. Thermodynamic limit

Theoretically, critical phenomena can only emerge in the thermodynamic limit of an infinite number of particles. For extended systems (e.g., a lattice with L sites), the thermodynamic limit can be obtained by increasing to infinity the system size ($L \rightarrow \infty$). In a single bosonic resonator, we can use its infinite-dimensional Hilbert space to introduce the infinite number of photons necessary for criticality by an appropriate scaling of the parameters (see Refs. [5, 24, 31, 35, 71, 72]). Here, we can do it by introducing an effective parameter N , under which the number of photons transforms as $n \rightarrow Nn$. Accordingly, $\{\Gamma, \xi, \eta\} \rightarrow \{\Gamma, \xi, \eta/N\}$. One can interpret N as the number of resonators in a Bose-Hubbard lattice, where each site is subject to the dissipators \hat{L}_1 and \hat{L}_2 , but only the uniform Fourier mode $k = 0$ is subject to the incoherent drive \hat{L}_3 . In this case, Eq. (1) describes the dynamics of the uniform mode $k = 0$ of the lattice

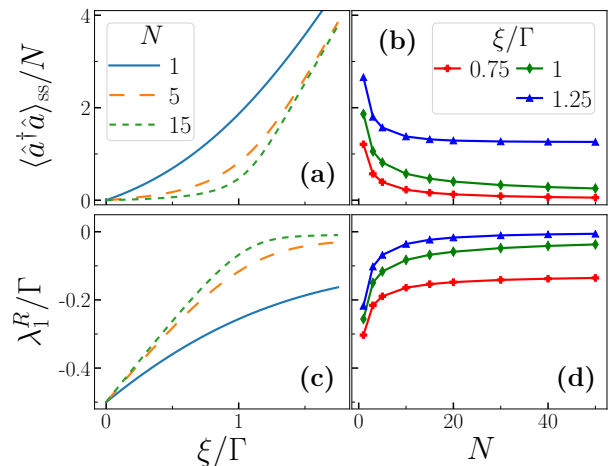


FIG. 1. Onset of the DPT in the R-frame for $\eta/\Gamma = 1$. (a) Steady-state rescaled number of photons $\langle \hat{a}^\dagger \hat{a} \rangle_{\text{ss}}/N$ versus the incoherent drive strength ξ/Γ for different values of the rescaling parameter N (the thermodynamic limit is $N \rightarrow \infty$). (b) $\langle \hat{a}^\dagger \hat{a} \rangle_{\text{ss}}/N$ as a function of N for different ξ : $\xi/\Gamma = 0.75$ (before the DPT), $\xi/\Gamma = 1$ (critical point), and $\xi/\Gamma = 1.25$ (after the DPT). (c) Liouvillian gap λ_1^R (in units of the damping rate Γ) versus ξ/Γ for different values of N . (d) λ_1^R as a function of N .

(see Appendix C). The dimensionless parameter N induces a scale transformation that keeps unchanged the typical photon lifetime $1/\Gamma$. Thus, we use Γ as a unit to study this problem.

B. Phase transition in the rotating frame

In Fig. 1, we show the onset of the transition for the R-frame Liouvillian \mathcal{L}^R (the data are obtained by an exact diagonalization of \mathcal{L}^R). As we see from Fig. 1(a), the change in the steady-state rescaled number of photons (i.e., $\langle \hat{a}^\dagger \hat{a} \rangle_{\text{ss}}/N$) becomes more abrupt as we increase the value of the parameter N . In Fig. 1(b) we demonstrate that, by increasing N , $\langle \hat{a}^\dagger \hat{a} \rangle_{\text{ss}}/N$ flows to zero before the phase transition, and converge to a finite value after it. In Fig. 1(c), instead, we plot the Liouvillian gap in the rotating frame λ_1^R , showing that the sharper the change in the photon number, the smaller is the Liouvillian gap. In Fig. 1(d) we show that by increasing N the gap λ_1^R is nonzero before the phase transition, and it become zero after the critical point. We have also verified that, in each symmetry sector, there is an eigenvalue closing at the DPT [it can also be concluded from Fig. 2 using Eq. (7)]. Thus, the symmetry breaking is described by the simultaneous closure (in both real and imaginary parts) of infinitely many eigenvalues, one for each symmetry generator sector [5, 32, 34, 73].

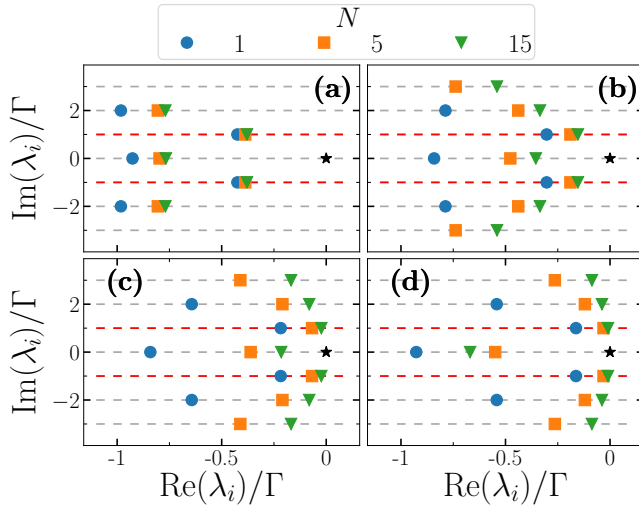


FIG. 2. Real and imaginary parts of the Liouvillian eigenvalues in the L-frame for $\omega_c/\Gamma = 1$, $\eta/\Gamma = 0.1$, and ξ/Γ equal to: (a) 0.25, (b) 0.75, (c) 1.25, (d) 1.75. Different markers represent different values of N , while the black stars represent the steady-state eigenvalue $\lambda_0 = 0$. The gray horizontal dashed lines represent $\text{Im}(\lambda_i) = k\omega_c$, where k is an integer. The red horizontal dashed lines indicate those eigenvalues associated to the Liouvillian gap. The choice $\omega_c/\Gamma = 1$ is arbitrary, and simply determines the imaginary part of λ_i .

C. Time crystal in the laboratory frame

Whereas in the R-frame the Liouvillian gap vanishes both in its real and imaginary parts ($\lambda_1^R \rightarrow 0$), in the L-frame the imaginary part of λ_1 is never zero, according to Eq. (7). That is, *the DPT in the R-frame implies a BTC in the L-frame*. The BTCs are, therefore, a critical phenomenon appearing only in the thermodynamic limit. Thus, we diagonalize the Liouvillian in the L-frame for increasing values of N for $\omega_c = \Gamma$. In Fig. 2 we plot the real and imaginary parts of the low-lying part of the spectrum for different values of ξ and N . As we enter the “broken-symmetry phase” and we increase N , there are slower and slower timescales, which are characterized by the imaginary parts of λ_i being multiples integer of ω_c , thus confirming Eq. (7). It follows that the field $\langle \hat{a} \rangle$ (and, thus, the electric field $\langle \hat{E} \rangle$) acquires an oscillatory behavior in the steady state in the thermodynamic limit. This can be interpreted as the emergence of a BTC [7]. Notice that this choice of ω_c is arbitrary and different values of ω_c would have produced time crystals characterised by a different frequency.

Time crystallization is also accompanied by a discontinuity in the photon number in $\hat{\rho}_{\text{ss}}$ [as given in Eq. (7), all the results for the steady state are identical in the two frames]. Indeed, $\langle \hat{a}^\dagger \hat{a} \rangle_{\text{ss}}$ in the L-frame is identical to that for the R-frame in Fig. 1(a). As such, the eigenvalue at $\text{Im}(\lambda_i) = 0$ plays a fundamental role: it is the one responsible for the non-analytical change of $\hat{\rho}_{\text{ss}}$ in the

L-frame [5].

D. Two-time correlation functions

The model under consideration displays a second-order DPT in the R-frame associated to the spontaneous symmetry breaking of $U(1)$ induced by the interplay of the nonlinear dissipation \hat{L}_2 and the incoherent drive \hat{L}_3 . However, in the L-frame a BTC manifests itself, by breaking both $U(1)$ and time-translation symmetries, similarly to those in Ref. [55]. Indeed, in the L-frame, some of the eigenvalues λ_i^R acquire an imaginary term proportional to $ik\omega_c$, according to Eq. (7). That is, Eq. (7) means that *the onset of a DPT in the R-frame corresponds to a BTC in the L-frame*.

We also stress that our model does not have a strong symmetry [64], even in the thermodynamic limit. Furthermore, there is no Hamiltonian coherent process taking place in a well-defined “decoherence-free subspace” [49, 57, 64, 74]. The emerging oscillations are the consequence of the same critical phenomenon leading to the $U(1)$ symmetry breaking, since both \mathcal{L} and \mathcal{L}^R are time-independent superoperators. This is the very same symmetry which allows to pass from one frame to the other without introducing any explicit time dependence in the Liouvillians.

The onset of DPTs can be visualized using quantum trajectory approaches [73, 75, 76] or by studying the dynamics of a properly initialized system [36, 77]. Finally, we stress that both DPT and BTC can be observed by two-time correlation measures which have already been employed in the study of DPTs [4]. In Figs. 3(a) and 3(b) we plot two-time correlation function in the L-frame steady state $C_{\text{ss}}^{(1)}(\tau) = \langle \hat{a}^\dagger(0)\hat{a}(\tau) \rangle_{\text{ss}}$. The long-lasting coherence time associated to an oscillatory behaviour is the proof of the emergence of a BTC. The abrupt increase in the amplitude of the oscillations demonstrates the emergence of the DPT. While $C_{\text{ss}}^{(1)}(\tau)$ exhibits oscillations at frequency ω_c , higher-order correlation functions can unveil those at multiple frequencies $k\omega_c$, $k \in \mathbb{N}$. For example, in Figs. 3(c) and 3(d) we plot the two-time correlation function $C_{\text{ss}}^{(2)}(\tau) = \langle \hat{a}^{\dagger 2}(0)\hat{a}^2(\tau) \rangle_{\text{ss}}$. We stress that $C_{\text{ss}}^{(2)} \neq g_{\text{ss}}^{(2)}$ due to the different ordering of the boson operators. This specific ordering in $C_{\text{ss}}^{(2)}$ allows one to observe the system oscillations frequency doubling those in Figs. 3(a) and 3(b).

IV. THE SCULLY-LAMB LASER MODEL

The above results regarding the DPT-BTC correspondence can be extended to other models characterized by a $U(1)$ symmetry and which obey Eq. (7). Here, we briefly show the emergence of the same phenomena in the celebrated Scully-Lamb laser model [59, 78, 79], whose

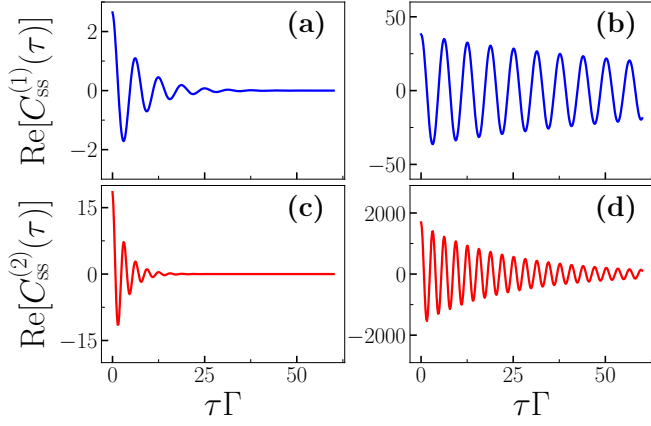


FIG. 3. Real part of the two-time correlation functions $C_{ss}^{(1)}(\tau)$ [(a) and (b)] and $C_{ss}^{(2)}(\tau)$ [(c) and (d)] vs delay time τ in the steady state for: (a, c) $\xi/\Gamma = 0.75$ (before the DPT); (b, d) $\xi/\Gamma = 1.25$ (after the DPT). Parameters: $\omega_c/\Gamma = 1$, $\eta/\Gamma = 0.1$, and $N = 30$.

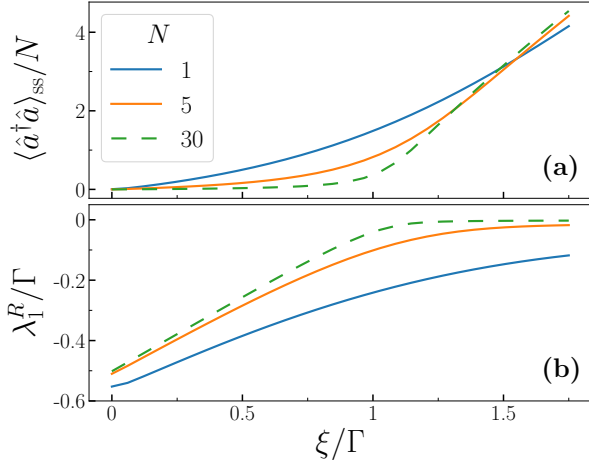


FIG. 4. Numerical study of the onset of the DPT in the R-frame for the Scully-Lamb model. (a): Rescaled number of photons $\langle \hat{a}^\dagger \hat{a} \rangle_{ss}/N$ as a function of the incoherent drive strength ξ/Γ . (b): Liouvillian gap λ_1^R (in units of the damping rate Γ) as a function of the incoherent drive ξ/Γ . Parameters: $\eta/\Gamma = 0.1$, $\beta/\Gamma = 0.005$.

Hamiltonian reads

$$\hat{H} = \omega_c \hat{a}^\dagger \hat{a}, \quad (8)$$

while the operators \hat{L}_j are

$$\hat{L}_1 = \hat{a}^\dagger (\sqrt{\xi} - \sqrt{\beta} \hat{a} \hat{a}^\dagger), \quad \hat{L}_2 = \sqrt{\eta} \hat{a} \hat{a}^\dagger, \quad \hat{L}_3 = \sqrt{\Gamma} \hat{a}, \quad (9)$$

where \hat{L}_1 describes a *nonlinear incoherent* drive (gain), \hat{L}_2 captures the nonlinear field decoherence, and \hat{L}_3 represents the single-particle loss. The parameter ξ represents the medium gain (incoherent drive) strength, β is the gain saturation (incoherent interaction) rate, η is the

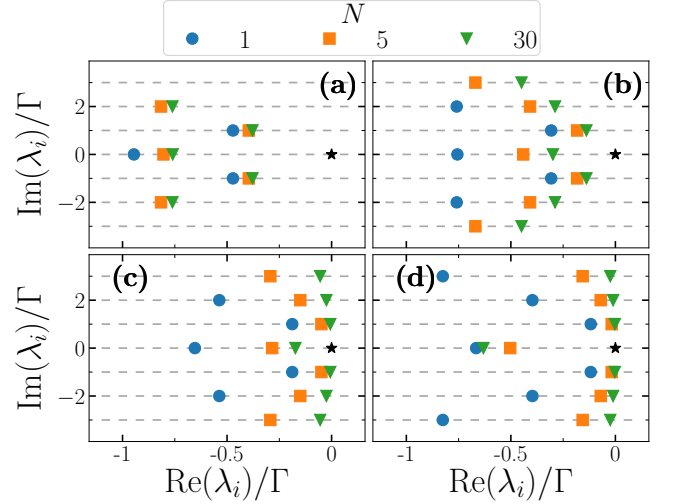


FIG. 5. Real and imaginary parts of the Liouvillian eigenvalues for the Scully-Lamb model in the L-frame for ξ/Γ equal to: (a) 0.25, (b) 0.75, (c) 1, (d) 1.5. Different markers represent different parameter N , while the black stars represent the steady-state eigenvalue $\lambda_0 = 0$. The gray horizontal dashed lines represent $\text{Im}(\lambda_i) = k\omega_c$, where k is an integer. The parameters used are: $\omega_c/\Gamma = 1$, $\eta/\Gamma = 0.1$, and $\beta/\Gamma = 0.005$.

decoherence rate, and Γ is the inverse of the photon lifetime.

Such a somewhat simplified model can be obtained from the full Scully-Lamb laser master equation [78] in the fourth-order field approximation, where $\xi = A$, $\beta = B^2/(4A)$ and $\eta = 3B/4$, with A and B being the laser gain and gain saturation parameters, respectively (see [79, 80]). Here, however, we consider β and η as independent parameters. To be physically meaningful, we must consider the weak gain-saturation regime, for which $\sqrt{\beta/\xi} \ll 1$. Away from this limit, the system may become unstable.

Similarly to the model in Sec. II, we can introduce the R-frame Liouvillian \mathcal{L}^R . Moreover, Eq. (7) remains valid also for this model.

To investigate criticality, we introduce the scaling as a function of the parameter N as $\{\xi, \Gamma, \eta, \beta\} \rightarrow \{\xi, \Gamma, \eta/N, \beta/N^2\}$. In Fig. 4, we show the onset of the transition for the R-frame Liouvillian \mathcal{L}^R as a function of N . Moreover, Fig. 5 demonstrate the emergence of a BTC, proving again the DPT-BTC correspondence.

These results generalize and support the findings of Ref. [59], by providing a genuine interpretation of the well-known lasing transition [17] in a more general framework, by explicitly taking into account the symmetries of the model and the spectral properties of the Liouvillian.

V. CONCLUSIONS

In this article, we have studied the emergence of a DPT and a BTC in a nonlinear optical model, where the nonlinearity comes from a dissipative term. To show these effects, we have analyzed the corresponding Lindblad-type Liouvillian superoperator and its spectrum for the studied system.

We have shown that, in the thermodynamic limit, a second-order DPT in the R-frame corresponds to a BTC in the L-frame. The two phenomena are the same in terms of the Liouvillian spectrum (or its gap) but just presented in different representations (frames). We find this prediction as the most important result of the manuscript. Moreover, Eq. (7) is an indirect proof of the existence of time crystallization in open quantum systems, since it connects BTCs' existence to that of second-order DPTs.

Beyond the interest in this correspondence, the novelty of the DPT discussed here is the *incoherent* nature of all the processes involved. Indeed, the system studied in Refs. [24, 71] was a single Kerr resonator coherently driven, while in Ref. [26] the incoherent (thermal-like) injection of photons was counterbalanced by a coherent two-body interaction process. Meaning that, in all these previous models, the system nonlinearity has been induced solely by a *coherent* interaction term, which is not the case for our model. This system can be realized with present technologies, such as in a incoherently driven engineered superconducting resonator [60, 61].

Differently from Ref. [49], the example shown here does not admit mixed coherences through which a dark Hamiltonian can produce oscillations. It is the incoherent injection of photons leading to multiple symmetry-breaking steady states which permit the presence of everlasting oscillations. Moreover, contrary to Ref. [7], the presence of strong dissipative processes does not prevent crystallization. Since the emergence of a BTC is intertwined to the emergence of a symmetry-breaking DPT, the BTC discussed here is a critical phenomenon. The extension of these results to other types of symmetries is one of the perspectives of this work.

The inclusion of nonlinear $U(1)$ Hamiltonian processes is straightforward, and allows to manipulate the time crystal oscillation periods. For example, by including Kerr-type nonlinearities the Liouvillian eigenvalues become not-equidistant and the resulting time crystals can have incommensurable oscillations. This will be the topic of future works.

Finally, this article prompts the question of the existence of a similar transformation in different symmetric systems, allowing to reinterpret the appearance of a BTC as the physics of a DPT, but just in a generalized “rotating frame”. Accordingly, emergent symmetries may be a key concept in understanding the physics of BTCs.

ACKNOWLEDGMENTS

The authors acknowledge the critical reading of Marcello Dalmonte, Simone Felicetti, and Vincenzo Macrì. The authors are grateful to the RIKEN Advanced Center for Computing and Communication (ACCC) for the allocation of computational resources of the RIKEN supercomputer system (HOKUSAI BigWaterfall). I.A. thanks the Grant Agency of the Czech Republic (Project No. 18-08874S), and Project no. CZ.02.1.010.00.016.0190000754 of the Ministry of Education, Youth and Sports of the Czech Republic. A.M. is supported by the Polish National Science Centre (NCN) under the Maestro Grant No. DEC-2019/34/A/ST2/00081. F.N. is supported in part by: NTT Research, Army Research Office (ARO) (Grant No. W911NF-18-1-0358), Japan Science and Technology Agency (JST) (via Q-LEAP and the CREST Grant No. JPMJCR1676), Japan Society for the Promotion of Science (JSPS) (via the KAKENHI Grant No. JP20H00134, and the JSPS-RFBR Grant No. JPJSBP120194828), and the Grant No. FQXi-IAF19-06 from the Foundational Questions Institute Fund (FQXi), a donor advised fund of the Silicon Valley Community Foundation.

Appendix A: Properties of Liouvillian symmetries

The Lindblad master equation, given in Eq. (??) is invariant under any transformation $\hat{a} \rightarrow \hat{a} \exp(i\phi)$ for an arbitrary real number ϕ . Thus, the model exhibits the $U(1)$ symmetry and the superoperator \mathcal{U} , defined as

$$\mathcal{U}\hat{\rho}(t) = \exp(-i\phi\hat{a}^\dagger\hat{a})\hat{\rho}(t)\exp(i\phi\hat{a}^\dagger\hat{a}), \quad (\text{A1})$$

commutes with the Liouvillian: $[\mathcal{L}, \mathcal{U}] = 0$.

While Liouvillian symmetries are not all associated to conserved quantities [62–64], they still constrain the system dynamics. Indeed, all the eigenmatrices of \mathcal{L} must be eigenmatrices of \mathcal{U} , that is,

$$\mathcal{U}\hat{\rho}_i = u_i\hat{\rho}_i, \quad (\text{A2})$$

where u_i is an eigenvalue of \mathcal{U} [5, 62, 64, 74].

The span of all the eigenmatrices $\hat{\rho}_i$ with the same u_i , such that

$$\mathcal{L}\hat{\rho}_i = u_i\hat{\rho}_i, \quad (\text{A3})$$

defines a *symmetry sector*. Each symmetry sector represents a part of the Liouvillian space which is not connected to its other parts (sectors) by the Liouvillian dynamics.

To better grasp the meaning of this symmetry, let us express the eigenmatrix $\hat{\rho}_i$ in the number (Fock) basis as

$$\hat{\rho}_i = \sum_{m,n} c_{m,n} |m\rangle\langle n|. \quad (\text{A4})$$

By combining Eqs. (A1), (A2), and (A4), one obtains

$$\begin{aligned}\mathcal{U}\hat{\rho}_i &= \sum_{m,n} c_{m,n} e^{-i\phi\hat{a}^\dagger\hat{a}} |m\rangle\langle n| e^{i\phi\hat{a}^\dagger\hat{a}} \\ &= \sum_{m,n} c_{m,n} e^{-i\phi(m-n)} |m\rangle\langle n| = u_i \hat{\rho}_i.\end{aligned}\quad (\text{A5})$$

We conclude that $\exp[-i\phi(m-n)]$ must be a constant and, therefore, any eigenmatrix $\hat{\rho}_i$ in Eq. (A4) must obey

$$\hat{\rho}_i = \sum_m c_m |m\rangle\langle m-k|, \quad (\text{A6})$$

for some constant integer $k \in \mathbb{Z}$. In other words, $\hat{\rho}_i$ must be an operator containing elements only on one diagonal, and different symmetry sectors occupy different upper and lower diagonals.

Appendix B: Proof of Eq. (7)

We can eliminate the Hamiltonian dependence of the Liouvillian by choosing the frame which rotates at the cavity frequency (the R-frame), i.e., the one rotating at the cavity frequency ω_c . The density matrix in the R-frame is

$$\hat{\rho}^R(t) = \exp(i\omega_c t \hat{a}^\dagger \hat{a}) \hat{\rho}(t) \exp(-i\omega_c t \hat{a}^\dagger \hat{a}). \quad (\text{B1})$$

We notice that, since all the dissipators are $U(1)$ -symmetric and the rotation is equivalent to applying the symmetry superoperator \mathcal{U} with $\phi = \omega_c t$, the dissipators are unchanged by the transformation. Hence, the Liouvillian in the R-frame is

$$\partial_t \hat{\rho}^R(t) = \mathcal{L}^R \hat{\rho}^R(t) = \left(\mathcal{D}[\hat{L}_1] + \mathcal{D}[\hat{L}_2] + \mathcal{D}[\hat{L}_3] \right) \hat{\rho}^R(t). \quad (\text{B2})$$

Having introduced the R-frame Liouvillian \mathcal{L}^R , we can introduce its eigenvalues λ_i^R and eigenvectors $\hat{\rho}_i^R$ defined by

$$\mathcal{L}^R \hat{\rho}_i^R = \lambda_i^R \hat{\rho}_i^R. \quad (\text{B3})$$

Notice that \mathcal{L}^R has exactly the same symmetries of the original problem, since $[\mathcal{U}, \mathcal{L}^R] = 0$. Thus, the condition in Eq. (A6) remains valid also for $\hat{\rho}_i^R$, i.e.,

$$\hat{\rho}_i^R = \sum_p c_p |p\rangle\langle p-k|. \quad (\text{B4})$$

Also note that, due to the super- and sub-diagonal form of $\hat{\rho}_i^R$ in Eq. (B4), the eigenmatrices $\hat{\rho}_i^R$ are, in general, non-Hermitian. This means that the corresponding eigenvalues λ_i^R are, in general, complex.

For a generic model and a generic change of reference, there is no trivial correspondence between λ_i^R and λ_i , as

well as $\hat{\rho}_i$ and $\hat{\rho}_i^R$. However, for the model under consideration we have

$$\begin{aligned}\mathcal{L} \hat{\rho}_i^R &= \mathcal{L}^R \hat{\rho}_i^R - i\omega_c [\hat{a}^\dagger \hat{a}, \hat{\rho}_i^R] \\ &= \lambda_i^R \hat{\rho}_i^R - i\omega_c \sum_p c_p [\hat{a}^\dagger \hat{a}, |p\rangle\langle p-k|] \\ &= \lambda_i^R \hat{\rho}_i^R - i\omega_c k \sum_p c_p |p\rangle\langle p-k| \\ &= (\lambda_i^R - i\omega_c k) \hat{\rho}_i^R,\end{aligned}\quad (\text{B5})$$

where the latter follows from Eq. (B4), with k an integer number. Thus, we have proved the following fundamental equalities:

$$\hat{\rho}_i = \hat{\rho}_i^R, \quad \lambda_i = \lambda_i^R - i\omega_c k. \quad (\text{B6})$$

This is exactly Eq. (7).

Appendix C: Thermodynamic limit of a single bosonic cavity

To grasp the correct scaling towards the thermodynamic limit, we can consider the semiclassical equation of motion and search for that scaling of the parameters under which $n \rightarrow Nn$, as detailed in Ref. [71]. Any transformations $\{\Gamma, \xi, \eta\} \rightarrow \{N^\mu \Gamma, N^\mu \xi, \eta/N^{1-\mu}\}$, for arbitrary μ , respect the photon number scaling $n \rightarrow Nn$, but only $\mu = 2$ is physically meaningful. Indeed, for any $\mu \neq 0$, the convergence towards the steady state becomes faster (or slower) for $\xi = 0$. Equivalently, the natural timescale of the problem, which is given by the photon-dissipation rate Γ , should not be modified by increasing the system size.

A different argument can be provided by considering a lattice of resonators:

$$\hat{H} = \omega_c \sum_{i=1}^N \hat{a}_i^\dagger \hat{a}_i + J \sum_{\langle i,j \rangle} \hat{a}_i^\dagger \hat{a}_j, \quad (\text{C1})$$

where $\langle i,j \rangle$ indicates that the sum runs over the nearest neighbours. Note that this Hamiltonian includes the J term and, thus, it is more general than that considered in Sec. II. The corresponding Liouvillian reads

$$\begin{aligned}\mathcal{L} \hat{\rho}(t) &= -i [\hat{H}, \hat{\rho}(t)] + \mathcal{D} \left[\sum_{i=1}^N \sqrt{\frac{\xi}{N}} \hat{a}_i^\dagger \right] \\ &\quad + \sum_{i=1}^N \left(\mathcal{D} [\sqrt{\Gamma} \hat{a}_i] + \mathcal{D} [\sqrt{\eta} \hat{a}_i^2] \right) \hat{\rho}(t).\end{aligned}\quad (\text{C2})$$

Notice the fundamental difference between $\mathcal{D} [\sum_i \hat{L}_i]$ and $\sum_i \mathcal{D} [\hat{L}_i]$. Indeed, in this model we are assuming that every cavity is identical, but while photonic emission is not correlated, the incoherent drive is only in the uniform mode of the cavity.

In the momentum space the Hamiltonian and dissipators are

$$\begin{aligned}
 \hat{H} &= \sum_k [\omega_c - 2J \cos(k)] \hat{a}_k^\dagger \hat{a}_k, \\
 \sum_i \mathcal{D} [\sqrt{\Gamma} \hat{a}_i] &= \sum_k \mathcal{D} [\sqrt{\Gamma} \hat{a}_k], \\
 \mathcal{D} \left[\sum_{i=1}^N \sqrt{\frac{\xi}{N}} \hat{a}_i^\dagger \right] &= \sum_k \mathcal{D} [\sqrt{\xi} \hat{a}_k^\dagger], \\
 \sum_i \mathcal{D} [\sqrt{\eta} \hat{a}_i^2] &= \frac{\xi}{N} \sum_{k,k',q} \mathcal{D} [\hat{a}_{k+q} \hat{a}_{k'-q}; \hat{a}_k^\dagger \hat{a}_{k'}^\dagger],
 \end{aligned} \tag{C3}$$

where $\mathcal{D} [\hat{A}, \hat{B}] = \hat{A} \cdot \hat{B} - \frac{1}{2}(\hat{A}\hat{B} \cdot + \cdot \hat{A}\hat{B})$ is the gen-

eralized Lindblad dissipator, and \cdot is the placeholder for the density matrix [e.g., $(\hat{A} \cdot \hat{B})\hat{\rho}(t) = \hat{A}\hat{\rho}(t)\hat{B}$]. For a large N , the effect of η is vanishingly small. Nevertheless, we cannot neglect it, since it is the dominant term in the phase with a large number of photons. However, we may effectively decouple the mode for $k = 0$ (the only driven one) from those of the other modes. The resulting model is that provided in Eq. (1), whose scaling with the parameter N is $\{\Gamma, \xi, \eta\} \rightarrow \{\Gamma, \xi, \eta/N\}$.

-
- [1] C. L. Kane and E. J. Mele, *Z₂ Topological Order and the Quantum Spin Hall Effect*, *Phys. Rev. Lett.* **95**, 146802 (2005).
- [2] J. Maldacena, *The Large- N Limit of Superconformal Field Theories and Supergravity*, *Int. J. Theor. Phys.* **38**, 1113 (1999).
- [3] H. J. Carmichael, *Breakdown of Photon Blockade: A Dissipative Quantum Phase Transition in Zero Dimensions*, *Phys. Rev. X* **5**, 031028 (2015).
- [4] T. Fink, A. Schade, S. Höfling, C. Schneider, and A. Imamoglu, *Signatures of a dissipative phase transition in photon correlation measurements*, *Nature Physics* **14**, 365 (2018).
- [5] F. Minganti, A. Biella, N. Bartolo, and C. Ciuti, *Spectral theory of Liouvillians for dissipative phase transitions*, *Phys. Rev. A* **98**, 042118 (2018).
- [6] The name boundary time crystals is used in Refs. [7, 8] as a synonym of dissipative time crystal. Indeed, a dissipative system can be seen as the boundary of the universe (where the universe is the sum of the system and its environment). Tracing out all the degrees of freedom of the environment, the boundary time crystals emerge.
- [7] F. Iemini, A. Russomanno, J. Keeling, M. Schirò, M. Dalmonte, and R. Fazio, *Boundary Time Crystals*, *Phys. Rev. Lett.* **121**, 035301 (2018).
- [8] C. Lledó and M. H. Szymańska, *Dissipative time crystal with or without Z₂ symmetry breaking*, *New Journal of Physics* (2020).
- [9] I. Carusotto and C. Ciuti, *Quantum fluids of light*, *Rev. Mod. Phys.* **85**, 299.
- [10] A. F. Kockum, A. Miranowicz, S. De Liberato, S. Savasta, and F. Nori, *Ultrastrong coupling between light and matter*, *Nat. Rev. Phys.* **1**, 19 (2019).
- [11] A. Delteil, T. Fink, A. Schade, S. Höfling, C. Schneider, and A. Imamoglu, *Towards polariton blockade of confined exciton-polaritons*, *Nature Materials* **18**, 219 (2019).
- [12] J. Q. You and F. Nori, *Atomic physics and quantum optics using superconducting circuits*, *Nature (London)* **474**, 589 (2011).
- [13] X. Gu, A. F. Kockum, A. Miranowicz, Y. X. Liu, and F. Nori, *Microwave photonics with superconducting quantum circuits*, *Phys. Rep.* **718-719**, 1 (2017).
- [14] M. Kjaergaard, M. E. Schwartz, J. Braumüller, P. Krantz, J. I.-J. Wang, S. Gustavsson, and W. D. Oliver, *Superconducting Qubits: Current State of Play*, *Annu. Rev. Condens. Matter Phys.* **11**, 369 (2020).
- [15] H. Breuer and F. Petruccione, *The Theory of Open Quantum Systems* (Oxford University Press, Oxford, 2007).
- [16] D. A. Lidar, *Lecture Notes on the Theory of Open Quantum Systems*, [arXiv:1902.00967](https://arxiv.org/abs/1902.00967).
- [17] V. DeGiorgio and M. O. Scully, *Analogy between the Laser Threshold Region and a Second-Order Phase Transition*, *Phys. Rev. A* **2**, 1170 (1970).
- [18] R. Bonifacio, M. Gronchi, and L. A. Lugiato, *Photon statistics of a bistable absorber*, *Phys. Rev. A* **18**, 2266 (1978).
- [19] B. R. Mollow and R. J. Glauber, *Quantum Theory of Parametric Amplification. I*, *Phys. Rev.* **160**, 1076 (1967).
- [20] P. Drummond and H. Carmichael, *Volterra cycles and the cooperative fluorescence critical point*, *Opt. Commun.* **27**, 160 (1978).
- [21] H. Weimer, *Variational Principle for Steady States of Dissipative Quantum Many-Body Systems*, *Phys. Rev. Lett.* **114**, 040402 (2015).
- [22] J. J. Mendoza-Arenas, S. R. Clark, S. Felicetti, G. Romero, E. Solano, D. G. Angelakis, and D. Jaksch, *Beyond mean-field bistability in driven-dissipative lattices: Bunching-antibunching transition and quantum simulation*, *Phys. Rev. A* **93**, 023821 (2016).
- [23] W. Casteels, F. Storme, A. Le Boité, and C. Ciuti, *Power laws in the dynamic hysteresis of quantum nonlinear photonic resonators*, *Phys. Rev. A* **93**, 033824 (2016).
- [24] N. Bartolo, F. Minganti, W. Casteels, and C. Ciuti, *Exact steady state of a Kerr resonator with one- and two-photon driving and dissipation: Controllable Wigner-function multimodality and dissipative phase transitions*, *Phys. Rev. A* **94**, 033841 (2016).
- [25] M. Foss-Feig, P. Niroula, J. T. Young, M. Hafezi, A. V. Gorshkov, R. M. Wilson, and M. F. Maghrebi, *Emergent equilibrium in many-body optical bistability*, *Phys. Rev. A* **95**, 043826 (2017).
- [26] A. Biella, F. Storme, J. Lebreuilly, D. Rossini, R. Fazio, I. Carusotto, and C. Ciuti, *Phase diagram of incoherently driven strongly correlated photonic lattices*, *Phys. Rev. A* **96**, 023839 (2017).

- [27] V. Savona, *Spontaneous symmetry breaking in a quadratically driven nonlinear photonic lattice*, *Phys. Rev. A* **96**, 033826 (2017).
- [28] T. E. Lee, S. Gopalakrishnan, and M. D. Lukin, *Unconventional Magnetism via Optical Pumping of Interacting Spin Systems*, *Phys. Rev. Lett.* **110**, 257204 (2013).
- [29] J. Jin, A. Biella, O. Viyuela, L. Mazza, J. Keeling, R. Fazio, and D. Rossini, *Cluster Mean-Field Approach to the Steady-State Phase Diagram of Dissipative Spin Systems*, *Phys. Rev. X* **6**, 031011 (2016).
- [30] R. Rota, F. Storme, N. Bartolo, R. Fazio, and C. Ciuti, *Critical behavior of dissipative two-dimensional spin lattices*, *Phys. Rev. B* **95**, 134431 (2017).
- [31] M.-J. Hwang, P. Rabl, and M. B. Plenio, *Dissipative phase transition in the open quantum Rabi model*, *Phys. Rev. A* **97**, 013825 (2018).
- [32] R. Rota, F. Minganti, A. Biella, and C. Ciuti, *Dynamical properties of dissipative XYZ Heisenberg lattices*, *New J. Phys.* **20**, 045003 (2018).
- [33] R. Rota, F. Minganti, C. Ciuti, and V. Savona, *Quantum Critical Regime in a Quadratically Driven Nonlinear Photonic Lattice*, *Phys. Rev. Lett.* **122**, 110405 (2019).
- [34] D. Huybrechts, F. Minganti, F. Nori, M. Wouters, and N. Shammah, *Validity of mean-field theory in a dissipative critical system: Liouvillian gap, $\mathbb{P}\mathbb{T}$ -symmetric anti-gap, and permutational symmetry in the XYZ model*, *Phys. Rev. B* **101**, 214302 (2020).
- [35] L. Garbe, M. Bina, A. Keller, M. G. A. Paris, and S. Felicetti, *Critical Quantum Metrology with a Finite-Component Quantum Phase Transition*, *Phys. Rev. Lett.* **124**, 120504 (2020).
- [36] H. Landa, M. Schiró, and G. Misguich, *Multistability of Driven-Dissipative Quantum Spins*, *Phys. Rev. Lett.* **124**, 043601 (2020).
- [37] J. B. Curtis, I. Boettcher, J. T. Young, M. F. Maghrebi, H. Carmichael, A. V. Gorshkov, and M. Foss-Feig, *Critical Theory for the Breakdown of Photon Blockade* (2020), [arXiv:2006.05593](https://arxiv.org/abs/2006.05593).
- [38] M. Fitzpatrick, N. M. Sundaresan, A. C. Y. Li, J. Koch, and A. A. Houck, *Observation of a Dissipative Phase Transition in a One-Dimensional Circuit QED Lattice*, *Phys. Rev. X* **7**, 011016 (2017).
- [39] M. Müller, S. Diehl, G. Pupillo, and P. Zoller, *Engineered Open Systems and Quantum Simulations with Atoms and Ions*, *Adv. At. Mol. Opt. Phys.* **61**, 1 (2012).
- [40] H. Bernien, S. Schwartz, A. Keesling, H. Levine, A. Omran, H. Pichler, S. Choi, A. S. Zibrov, M. Endres, M. Greiner, V. Vuletić, and M. D. Lukin, *Probing many-body dynamics on a 51-atom quantum simulator*, *Nature (London)* **551**, 579 (2017).
- [41] M. Aspelmeyer, T. J. Kippenberg, and F. Marquardt, *Cavity optomechanics*, *Rev. Mod. Phys.* **86**, 1391 (2014).
- [42] E. Gil-Santos, M. Labousse, C. Baker, A. Goetschy, W. Hease, C. Gomez, A. Lemaître, G. Leo, C. Ciuti, and I. Favero, *Light-Mediated Cascaded Locking of Multiple Nano-Optomechanical Oscillators*, *Phys. Rev. Lett.* **118**, 063605 (2017).
- [43] J. Kasprzak, M. Richard, S. Kundermann, A. Baas, P. Jeambrun, J. M. J. Keeling, F. M. Marchetti, M. H. Szymanska, R. Andre, J. L. Staehli, V. Savona, P. B. Littlewood, B. Deveaud, and L. S. Dang, *Bose-Einstein condensation of exciton polaritons*, *Nature (London)* **443**, 409 (2006).
- [44] J. M. Fink, A. Dombi, A. Vukics, A. Wallraff, and P. Domokos, *Observation of the Photon-Blockade Breakdown Phase Transition*, *Phys. Rev. X* **7**, 011012 (2017).
- [45] S. R. K. Rodriguez, W. Casteels, F. Storme, N. Carlon Zambon, I. Sagnes, L. Le Gratiet, E. Galopin, A. Lemaître, A. Amo, C. Ciuti, and J. Bloch, *Probing a Dissipative Phase Transition via Dynamical Optical Hysteresis*, *Phys. Rev. Lett.* **118**, 247402 (2017).
- [46] N. Shammah, S. Ahmed, N. Lambert, S. De Liberato, and F. Nori, *Open quantum systems with local and collective incoherent processes: Efficient numerical simulations using permutational invariance*, *Phys. Rev. A* **98**, 063815 (2018).
- [47] K. Tucker, B. Zhu, R. J. Lewis-Swan, J. Marino, F. Jimenez, J. G. Restrepo, and A. M. Rey, *Shattered time: can a dissipative time crystal survive many-body correlations?*, *New J. Phys.* **20**, 123003 (2018).
- [48] C. Lledó, T. K. Mavrogordatos, and M. H. Szymańska, *Driven Bose-Hubbard dimer under nonlocal dissipation: A bistable time crystal*, *Phys. Rev. B* **100**, 054303 (2019).
- [49] B. Buča, J. Tindall, and D. Jaksch, *Non-stationary coherent quantum many-body dynamics through dissipation*, *Nat. Commun.* **10**, 1730 (2019).
- [50] K. Seibold, R. Rota, and V. Savona, *Dissipative time crystal in an asymmetric nonlinear photonic dimer*, *Phys. Rev. A* **101**, 033839 (2020).
- [51] K. Sacha and J. Zakrzewski, *Time crystals: a review*, *Rep. Prog. Phys.* **81**, 016401 (2017).
- [52] Z. Gong, R. Hamazaki, and M. Ueda, *Discrete Time-Crystalline Order in Cavity and Circuit QED Systems*, *Phys. Rev. Lett.* **120**, 040404 (2018).
- [53] A. Riera-Campenay, M. Moreno-Cardoner, and A. Sanpera, *Time crystallinity in open quantum systems*, *Quantum* **4**, 270 (2020).
- [54] F. M. Gambetta, F. Carollo, M. Marcuzzi, J. P. Garrahan, and I. Lesanovsky, *Discrete Time Crystals in the Absence of Manifest Symmetries or Disorder in Open Quantum Systems*, *Phys. Rev. Lett.* **122**, 015701 (2019).
- [55] O. Scarlatella, R. Fazio, and M. Schiró, *Emergent finite frequency criticality of driven-dissipative correlated lattice bosons*, *Phys. Rev. B* **99**, 064511 (2019).
- [56] E. M. Kessler, G. Giedke, A. Imamoglu, S. F. Yelin, M. D. Lukin, and J. I. Cirac, *Dissipative phase transition in a central spin system*, *Phys. Rev. A* **86**, 012116 (2012).
- [57] C. Booker, B. Buča, and D. Jaksch, *Non-stationarity and Dissipative Time Crystals: Spectral Properties and Finite-Size Effects*, (2020), [arXiv:2005.05062](https://arxiv.org/abs/2005.05062).
- [58] J. Lebreuilly, A. Biella, F. Storme, D. Rossini, R. Fazio, C. Ciuti, and I. Carusotto, *Stabilizing strongly correlated photon fluids with non-Markovian reservoirs*, *Phys. Rev. A* **96**, 033828 (2017).
- [59] N. Takemura, M. Takiguchi, and M. Notomi, *Low- and high- β lasers in Class-A limit: photon statistics, linewidth, and the laser-phase transition analogy*, (2019), [arXiv:1904.01743](https://arxiv.org/abs/1904.01743).
- [60] Z. Leghtas, S. Touzard, I. M. Pop, A. Kou, B. Vlastakis, A. Petrenko, K. M. Sliwa, A. Narla, S. Shankar, M. J. Hatridge, M. Reagor, L. Frunzio, R. J. Schoelkopf, M. Mirrahimi, and M. H. Devoret, *Confining the state of light to a quantum manifold by engineered two-photon loss*, *Science* **347**, 853 (2015).
- [61] R. Lescanne, M. Villiers, T. Peronnin, A. Sarlette, M. Delbecq, B. Huard, T. Kontos, M. Mirrahimi, and Z. Leghtas, *Exponential suppression of bit-flips in a qubit encoded in an oscillator*, *Nature Physics* **16**, 509 (2020).

- [62] B. Baumgartner and N. Heide, *Analysis of quantum semigroups with GKS-Lindblad generators: II. General*, *J. Phys. A: Math. Theor.* **41**, 395303 (2008).
- [63] B. Buča and T. Prosen, *A note on symmetry reductions of the Lindblad equation: transport in constrained open spin chains*, *New J. Phys.* **14**, 073007 (2012).
- [64] V. V. Albert and L. Jiang, *Symmetries and conserved quantities in Lindblad master equations*, *Phys. Rev. A* **89**, 022118 (2014).
- [65] J. Johansson, P. Nation, and F. Nori, *QuTiP: An open-source Python framework for the dynamics of open quantum systems*, *Comp. Phys. Commun.* **183**, 1760 (2012).
- [66] J. Johansson, P. Nation, and F. Nori, *QuTiP 2: A Python framework for the dynamics of open quantum systems*, *Comp. Phys. Commun.* **184**, 1234 (2013).
- [67] H. Watanabe and M. Oshikawa, *Absence of Quantum Time Crystals*, *Phys. Rev. Lett.* **114**, 251603 (2015).
- [68] K. Sacha, *Modeling spontaneous breaking of time-translation symmetry*, *Phys. Rev. A* **91**, 033617 (2015).
- [69] S. Choi, J. Choi, R. Landig, G. Kucsko, H. Zhou, J. Isoya, F. Jelezko, S. Onoda, H. Sumiya, V. Khemani, C. von Keyserlingk, N. Y. Yao, E. Demler, and M. D. Lukin, *Observation of discrete time-crystalline order in a disordered dipolar many-body system*, *Nature (London)* **543**, 221 (2017).
- [70] J. Zhang, P. W. Hess, A. Kyprianidis, P. Becker, A. Lee, J. Smith, G. Pagano, I.-D. Potirniche, A. C. Potter, A. Vishwanath, N. Y. Yao, and C. Monroe, *Observation of a discrete time crystal*, *Nature (London)* **543**, 217 (2017).
- [71] W. Casteels and C. Ciuti, *Quantum entanglement in the spatial-symmetry-breaking phase transition of a driven-dissipative Bose-Hubbard dimer*, *Phys. Rev. A* **95**, 013812 (2017).
- [72] S. Felicetti and A. Le Boité, *Universal Spectral Features of Ultrastrongly Coupled Systems*, *Phys. Rev. Lett.* **124**, 040404 (2020).
- [73] J. Jin, A. Biella, O. Viyuela, C. Ciuti, R. Fazio, and D. Rossini, *Phase diagram of the dissipative quantum Ising model on a square lattice*, *Phys. Rev. B* **98**, 241108(R) (2018).
- [74] V. V. Albert, B. Bradlyn, M. Fraas, and L. Jiang, *Geometry and Response of Lindbladians*, *Phys. Rev. X* **6**, 041031 (2016).
- [75] N. Bartolo, F. Minganti, J. Lolli, and C. Ciuti, *Homodyne versus photon-counting quantum trajectories for dissipative Kerr resonators with two-photon driving*, *Eur. Phys. J. Spec. Top.* **226**, 2705 (2017).
- [76] F. Vicentini, F. Minganti, R. Rota, G. Orso, and C. Ciuti, *Critical slowing down in driven-dissipative Bose-Hubbard lattices*, *Phys. Rev. A* **97**, 013853 (2018).
- [77] H. Landa, M. Schiró, and G. Misguich, *Correlation-induced steady states and limit cycles in driven dissipative quantum systems*, (2020), [arXiv:2001.05474](https://arxiv.org/abs/2001.05474).
- [78] Y. Yamamoto and A. Imamoglu, *Mesoscopic Quantum Optics* (John Wiley and Sons, New York, 1999).
- [79] I. I. Arkhipov, A. Miranowicz, F. Minganti, and F. Nori, *Quantum and semiclassical exceptional points of a linear system of coupled cavities with losses and gain within the Scully-Lamb laser theory*, *Phys. Rev. A* **101**, 013812 (2020).
- [80] I. I. Arkhipov, A. Miranowicz, O. D. Stefano, R. Stassi, S. Savasta, F. Nori, and Ş. K. Özdemir, *Scully-Lamb quantum laser model for parity-time-symmetric whispering-gallery microcavities: Gain saturation effects and nonreciprocity*, *Phys. Rev. A* **99**, 042309 (2019).